

# Hydrogenation Properties of Vanadium-Based Alloys with Large Hydrogen Storage Capacity

M. Tsukahara\*

IMRA Material R&D Co., Ltd., Kariya 448-0032, Japan

Hydrogenation properties of the vanadium-rich ternary V-Ti-Cr alloy was investigated, which is of interest as a hydrogen carrier for fuel-cell vehicles. The dependence of hydrogen content of the hydrides with low plateau pressure ( $\beta$  phase) on the unit cell volume of the dehydrogenated alloys ( $\alpha$  phase) is found to be different from that of the hydrides ( $\gamma$  phase) with high plateau pressure. By optimizing the alloy composition, a large effective hydrogen storage capacity of 2.62 mass% is obtained. [doi:10.2320/matertrans.M2010216]

(Received June 23, 2010; Accepted October 14, 2010; Published December 1, 2010)

**Keywords:** vanadium-based alloy, hydrogen capacity, hydrogen storage, hydride, solid solution, titanium, chromium

## 1. Introduction

For fuel-cell vehicles, on-board hydrogen storage is a crucial technology, but suitable hydrogen carriers are not yet available. For example, although complex hydrides are expected to have large hydrogen mass capacity, their hydrogen volume capacity and cycle durability have not reached practically usable levels.

Conventional hydrogen-storage alloys have not met the required level of hydrogen mass capacity for on-board hydrogen storage. However, the application of hydrogen storage alloys to hybrid reservoirs has recently been examined<sup>1)</sup> because of its relative advantages of high hydrogen volume capacity, kinetics and cycle durability compared over complex hydrides. D. Mori *et al.* reported that, by using a hydrogen storage alloy with an effective hydrogen capacity of 3 mass%, the reservoir volume decreases to 83 L for on-board storage of 5 kg of hydrogen, which is considered to be a practical level for fuel-cell passenger vehicles.

Among conventional hydrogen storage alloys, body-centered cubic (BCC) solid solutions of V-based alloys with a large effective mass capacity near 3 mass%<sup>2-5)</sup> have been studied in particular. V-Ti-Cr alloys have attracted attention because the stability of these hydrides are adjustable by changing alloy composition and the effective hydrogen capacity is larger than 2.5 mass%.<sup>4,5)</sup>

Libowitz and Maeland<sup>6)</sup> reported that BCC alloys typically have two-step plateaus on the pressure-composition isotherms through formation of two different kinds of hydrides. In this publication, the original alloy (or dehydrogenated phase), the hydride with low plateau pressure and the hydride with high plateau pressure are defined as  $\alpha$  phase,  $\beta$  phase and  $\gamma$  phase, respectively, although, for evaluation, these phases are not necessarily to be a single phase.

Hydrogen content of  $\alpha$ ,  $\beta$  and  $\gamma$  phases are reported to be changed according to alloy composition of V-Ti alloy<sup>7)</sup> and V-Ti-Cr alloy.<sup>5)</sup> To increase the hydrogen capacity of vanadium-based alloys, influence of composition of alloy on hydrogen content of both of starting point of formation

and fully hydrogenated  $\gamma$  phase for V-rich V-Ti-Cr alloy was investigated. This publication presents results of the investigation of the crystal structures of the  $\alpha$ ,  $\beta$  and  $\gamma$  phases of V-Ti-Cr, and reports a large effective hydrogen capacity of 2.62 mass%.

## 2. Experimental Details

The constituent metals of vanadium flakes (purity 99% up), titanium wire (purity 99% up) and chromium lumps (purity 99.99%) were weighed to prepare the alloy according to the composition shown in Fig. 1. To obtain ingots, the constituents were melted by arc melting in a water-cooled copper furnace under argon gas at a pressure of  $5 \times 10^4$  Pa. After removing surface of the ingots, they were placed into a reactor and heated to a temperature below 673 K in a hydrogen atmosphere at lower than 1.0 MPa to be hydrogenated. Subsequently, they were mechanically crushed in air.

Pressure-composition isotherms (PCT curves) were measured with a Sievert's apparatus. Each powder sample was put into a SS316 reactor tube, which was evacuated and heated to 673 K. Hydrogen was introduced up to 3.3 MPa and the reactor tube was cooled to room temperature for initial activation. To obtain the hydrogen zero point of PCT curve, the specimen was dehydrogenated with a rotary pump at 673 K for longer than 8 h.

To verify the hydrogen content and crystal structure of  $\alpha$  phase and two hydrides ( $\beta$  phase and  $\gamma$  phase), each specimen was prepared using Sievert's apparatus, as described above. To obtain the  $\alpha$  phase specimens, the specimens were evacuated with a rotary pump at 673 K for longer than 8 h, cooled to room temperature and then air was introduced into the reactor tube. To obtain specimens of  $\beta$  phase with the hydrogen content just below the level at which the  $\gamma$  phase starts to form, the specimens were kept sufficiently long to attain equilibrium under conditions of hydrogen pressure and temperature obtained from the PCT curves shown in Table 1. Immediately after detachment of the reactor tube from the apparatus, acetone was introduced into it to prevent the specimen from dehydrogenating. In this publication, this specimen is simply called the  $\beta$  phase specimen, although it is not necessarily to be a single phase.

\*Present address: AISIN Seiki Co., Ltd., Kariya 448-8650, Japan

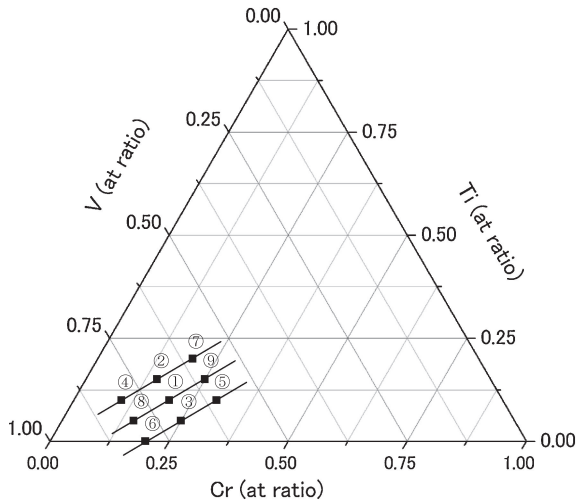


Fig. 1 V-Ti-Cr alloy used in this study (atomic ratio).

Table 1 Temperature and pressure equilibrium conditions for  $\beta$  phase hydride.

Sample Nr	Alloy composition (at%)			Equilibrium condition	
	V	Ti	Cr	Temperature (K)	Pressure (MPa)
1	70	10	20	333	0.0105
2	70	15	15	353	0.0156
3	70	5	25	253	0.0105
4	80	10	10	333	0.0195
5	60	10	30	293	0.0101
6	80	0	20	253	0.0111
7	60	20	20	373	0.0151
8	80	5	15	313	0.0109
9	60	15	25	353	0.0101

To obtain a  $\gamma$  phase sample, the reactor tube was left in the Sievert's apparatus sufficiently long to attain equilibrium at 233 K and 3.3 MPa, then the reactor tube was cooled by liquid nitrogen and detached from the apparatus. Immediately after detachment of the reactor tube from the apparatus, acetone was introduced into it with holding the reactor tube in liquid nitrogen to prevent dehydrogenation of the specimens.

The hydrogen content of each specimen was measured via the inert-gas fusion method (Japanese Industrial Standard JIS Z2614), and the crystal structure was determined by powder X-ray diffraction (XRD) using the Cu-K $\alpha$  line (Rigaku RAD-C).

### 3. Results and Discussion

#### 3.1 Influence of acetone immersion

The validity of acetone immersion to obtain specimens of  $\alpha$  phase after dehydrogenation and to obtain specimens of  $\gamma$  phase after hydrogenation was examined by using the 70 at% V-10 at% Ti-20 at% Cr alloy, for which the PCT curves are shown in Fig. 2.

The  $\alpha$  phase specimens were obtained by evacuation for 8 h at 673 K. The  $\gamma$  phase specimens saturated with hydrogen were obtained at 233 K and 3.3 MPa. Promptly after the

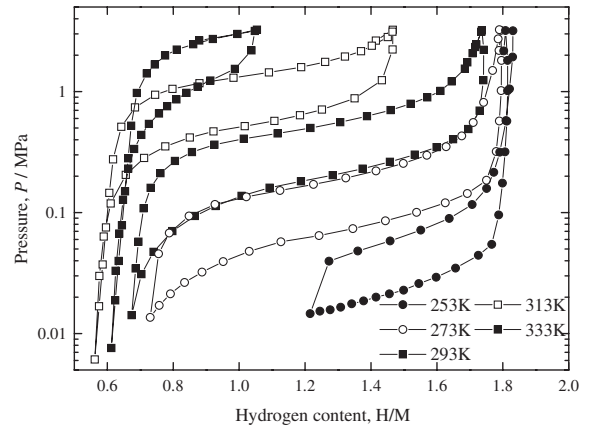


Fig. 2 Pressure composition-isotherms for 70 at% V-10 at% Ti-20 at% Cr.

Table 2 Hydrogen contents of  $\alpha$  and  $\gamma$  phases of V-10 at% Ti-20 at% Cr by PCT measurement and by inert-gas fusion method (FM) with acetone immersion and without acetone immersion.

	mass%	
	$\alpha$ phase	$\gamma$ phase
PCT measurement	0.0	3.6
With acetone immersion (FM)	0.028	3.45
Without acetone immersion (FM)	0.024	1.22

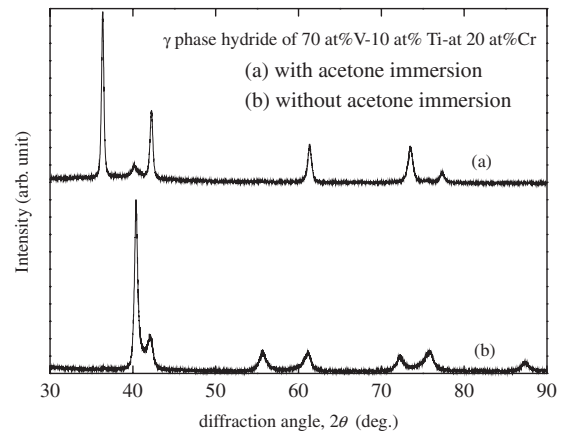


Fig. 3 Comparison of XRD profiles for  $\gamma$  phase hydride of V-10 at% Ti-20 at% Cr (a) with and (b) without acetone immersion.

reactor tubes were detached from the Sievert's apparatus, the specimens of  $\alpha$  and  $\gamma$  phases were subjected to acetone immersion. For comparison, the specimen without acetone immersion was also prepared. The hydrogen contents, obtained by PCT measurements and by inert-gas fusion, are given in Table 2. Hydrogen content of  $\alpha$  phase specimens was 0.028 and 0.024 mass% for acetone-treated and untreated samples, respectively. Both specimens are considered to be fully degassed. From this result, it is concluded that acetone does not increase hydrogen content in the specimen.

Hydrogen content of the  $\gamma$  phase specimen without acetone immersion is less than that of with acetone immersion. From the XRD data shown in Fig. 3, the specimen without acetone immersion is regarded as a single phase of monohydride with the BCT structure. Because the specimen temperature was

Table 3 Hydrogen content of  $\beta$  phase ( $C_{H_2}^\beta$ ) and  $\gamma$  phase ( $C_{H_2}^\gamma$ ) and effective hydrogen capacity ( $C_{H_2}^{\text{eff}}$ ).

Sample Nr.	Composition (at%)			Hydrogen content					
	V	Ti	Cr	(H/M)			(mass%)		
				$C_{H_2}^\beta$	$C_{H_2}^\gamma$	$C_{H_2}^{\text{eff}}$	$C_{H_2}^\beta$	$C_{H_2}^\gamma$	$C_{H_2}^{\text{eff}}$
1	70	10	20	0.62	1.86	1.24	1.22	3.65	2.43
2	70	15	15	0.69	1.87	1.18	1.36	3.69	2.33
3	70	5	25	0.53	0.97	0.44	1.04	1.89	0.85
4	80	10	10	0.76	1.88	1.12	1.49	3.71	2.22
5	60	10	30	0.56	1.47	0.91	1.10	2.88	1.78
6	80	0	20	0.56	0.85	0.29	1.09	1.67	0.58
7	60	20	20	0.71	1.74	1.03	1.40	3.44	2.04
8	80	5	15	0.65	1.84	1.19	1.28	3.68	2.40
9	60	15	25	0.59	1.92	1.33	1.16	3.78	2.62

maintained not lower than 303 K, at which the equilibrium pressure for the  $\gamma$  phase is sufficiently higher than 0.1 MPa (Fig. 2), under those conditions, the  $\gamma$  phase of dihydride changes into the single phase of monohydride by hydrogen discharging. However, the specimen treated with acetone consists of a face-centered cubic (FCC) phase<sup>2)</sup> and a body-centered tetragonal (BCT) phase,<sup>8)</sup> which are regarded as dihydride and monohydride, respectively. Acetone immersion would cause the alloy surface to be oxidized, and hence it serves as a barrier against dehydrogenation.

### 3.2 Hydrogen storage properties of V-rich V-Ti-Cr alloys

The effective hydrogen capacity is defined as the difference of the hydrogen content between the  $\gamma$  phase and the  $\beta$  phase of a specimen. From the PCT measurements, the effective hydrogen capacity was obtained for each specimen, with the results given in Table 3. In Fig. 4, these values are shown as a function of V content,  $C(V)$ , by  $C(\text{Cr}) - C(\text{Ti})$ , where  $C(X)$  is defined as the content of element X.

For  $C(\text{Cr}) - C(\text{Ti}) = 10 \text{ at\%}$ , the effective hydrogen capacity is rather large because the hydrogen content of the  $\gamma$  phase is large and that of the  $\beta$  phase is rather small (Fig. 4). The alloy of 60 at% V-15 at% Ti-25 at% Cr has a hydrogen capacity of 2.62 mass% (1.33 H/M), which is the largest among all the specimens in this study. However, for  $C(\text{Cr}) - C(\text{Ti}) = 0 \text{ at\%}$ . The effective hydrogen capacity is smaller compared to that of  $C(\text{Cr}) - C(\text{Ti}) = 10 \text{ at\%}$ , because the hydrogen content of the  $\beta$  phase is larger than that of  $C(\text{Cr}) - C(\text{Ti}) = 10 \text{ at\%}$ , in spite of the large hydrogen content of the  $\gamma$  phase. For  $C(\text{Cr}) - C(\text{Ti}) = 20 \text{ at\%}$ , although the hydrogen content of the  $\beta$  phase is small, the effective hydrogen capacity is small because the  $\gamma$  phase hydrogen content of those specimens is very small. Among all specimens of this study, the alloy of 80 at% V-20 at% Cr shows the smallest hydrogen capacity of 0.58 mass%.

### 3.3 Crystal structure of V-rich V-Ti-Cr alloys and their hydrides

Crystal structures and unit cell lengths of  $\alpha$ ,  $\beta$  and  $\gamma$  phases are given in Table 4. All dehydrogenated specimens ( $\alpha$  phase) show a single BCC phase and the unit cell length ranges from 0.300 to 0.305 nm, depending on the alloy

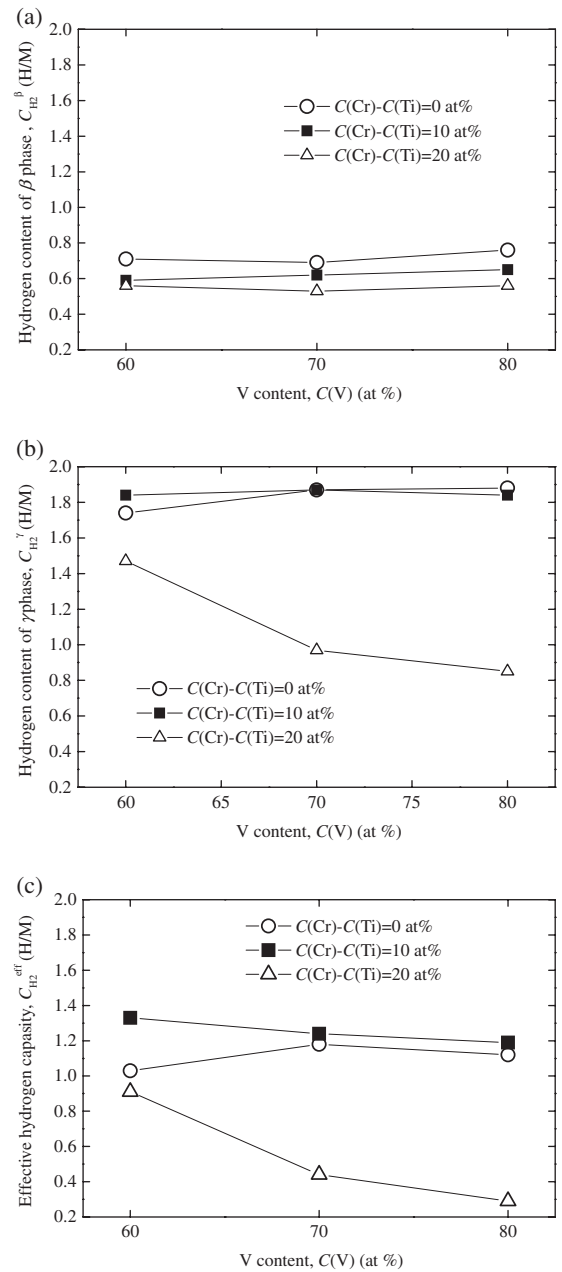
Fig. 4 Composition dependence of hydrogen contents of (a)  $\beta$  phase, (b)  $\gamma$  phase and (c) effective hydrogen capacity.

Table 4 Crystal structures of V-based alloys and hydrides. (nm)

Sample Nr.	$\alpha$ phase	$\beta$ phase		$\gamma$ phase				
	BCC	BCT		FCC(1)	BCT		FCC(2)	BCC
	$a$	$a$	$c$	$a$	$a$	$c$	$a$	$a$
1	0.302	0.304	0.328	0.428	0.303	0.334	—	—
2	0.304	0.313	0.321	0.429	0.303	0.339	—	—
3	0.300	0.301	0.328	0.429	0.300	0.333	0.398	0.280
4	0.304	0.307	0.333	0.428	0.303	0.340	—	—
5	0.301	0.303	0.326	0.427	0.301	0.328	0.397	0.281
6	0.300	0.299	0.329	0.429	0.300	0.333	0.398	0.280
7	0.305	0.314	0.319	0.430	0.304	0.333	—	—
8	0.303	0.302	0.332	0.428	0.303	0.356	—	—
9	0.302	0.305	0.323	0.428	0.303	0.333	—	—

Table 5 Change of volume per metal atom from  $\alpha$  phase and  $\beta$  phase to  $\gamma$  phase by hydrogenation. ( $10^{-3} \text{ nm}^3$ )

Sample Nr.	FCC(1)		BCT		FCC(2)		BCC	
	$V_\gamma/4$	$V_\gamma/4$	$V_\gamma/4$	$V_\gamma/4$	$V_\gamma/4$	$V_\gamma/4$	$V_\gamma/4$	$V_\gamma/4$
	$-V_\beta/2$	$-V_\alpha/2$	$-V_\beta/2$	$-V_\alpha/2$	$-V_\beta/2$	$-V_\alpha/2$	$-V_\beta/2$	$-V_\alpha/2$
1	4.5	5.8	0.2	1.6	—	—	—	—
2	4.0	5.6	-0.1	1.5	—	—	—	—
3	4.8	6.2	0.1	1.5	0.8	2.2	-3.9	-2.5
4	3.9	5.6	-0.1	1.6	—	—	—	—
5	4.6	5.8	0.0	1.3	0.8	2.1	-3.8	-2.5
6	5.0	6.3	0.2	1.5	1.0	2.3	-3.8	-2.5
7	4.1	5.7	-0.4	1.2	—	—	—	—
8	4.4	5.7	1.1	2.5	—	—	—	—
9	4.6	5.8	0.3	1.5	—	—	—	—

composition as per Vegard's Law. All  $\beta$  phase specimens were confirmed as a single BCT phase similar to the monohydride of pure vanadium.<sup>8)</sup>

In contrast, each  $\gamma$  phase specimen is multiphase, which includes at least one FCC and one BCT phase. The unit cell length of the  $\gamma$  BCT phase is nearly equal to that of the  $\beta$  BCT phase. Therefore, the  $\gamma$  BCT phase could be regarded as a monohydride, which is considered to have dehydrogenated in air from the  $\gamma$  phase in spite of acetone immersion.

For samples of  $C(\text{Cr}) - C(\text{Ti}) = 20 \text{ at}\%$ , the unit cell length of the  $\alpha$  phase is not longer than 0.301 nm. In this case, the  $\gamma$  phase accompanies with another FCC phase (called the secondary FCC phase) and a BCC phase. The secondary FCC phase has a smaller unit cell volume than that of the dominant FCC phase and the  $\gamma$  BCC phase has a smaller unit cell volume than that of the  $\alpha$  phase. By hydrogenation, the alloy decomposes into the small BCC phase and two hydrides with the FCC structure. The  $\alpha$  phase specimen was obtained by dehydrogenation after at least three sequences of hydrogenation. The XRD data show that the  $\alpha$  phase specimen consists of a single phase whereas some  $\gamma$  phase specimens contain two FCC hydrides and one BCC phase. By hydrogenation and dehydrogenation, disproportionation and recombination occur, respectively, and these reactions are reversible similar to super-laminate materials such as Mg-Cu and Mg-Pd.<sup>9,10)</sup>

In Table 5, average volume per metal atom in a unit cell of the  $\gamma$  phase ( $V_\gamma/4$ ) is compared with that of the  $\alpha$  phase ( $V_\alpha/2$ ) and the  $\beta$  phase ( $V_\beta/2$ ), where  $V_\alpha$ ,  $V_\beta$  and  $V_\gamma$  are

defined as unit cell volumes of  $\alpha$ ,  $\beta$  and  $\gamma$  phases, respectively. For the FCC phase, which has a larger average volume per metal atom, the difference of  $V_\gamma/4 - V_\alpha/2$  ranges from 0.056 to 0.062  $\text{nm}^3$ , whereas the difference  $V_\gamma/2 - V_\alpha/2$  ranges from 0.12 to 0.25  $\text{nm}^3$ . Therefore, the larger FCC phase is considered a dihydride phase akin to the dihydride of pure vanadium.<sup>2)</sup>

For  $C(\text{Cr}) - C(\text{Ti}) = 20 \text{ at}\%$ , the volume per metal atom of the secondary (i.e., smaller) FCC phase is nearly equal to that of the  $\beta$  BCT phase, and the secondary FCC phase undergoes a lattice expansion, magnitude of which is nearly half of the  $\alpha$  phase into the dominant (i.e., larger) FCC phase. Therefore, the secondary FCC phase is considered to be monohydride, just as for  $\text{CrH}^{11)}$  and  $\text{VCuNi}^{12)}$ . The  $\gamma$  BCC phase observed for  $C(\text{Cr}) - C(\text{Ti}) = 20 \text{ at}\%$  has a smaller volume per metal atom than those of the  $\alpha$  and  $\beta$  phases as described previously.

### 3.4 Relationship between unit cell size and hydrogen capacity

From a practical viewpoint, a large effective hydrogen capacity is desired for hydrogen storage materials. As discussed in the previous sections, the relationship between the hydrogen capacity of the  $\beta$  and  $\gamma$  phases and the alloy composition is important to obtain a large effective hydrogen storage capacity.

In Fig. 5(a) and (b), the relationship between the unit cell length of the  $\alpha$  phase and the hydrogen content of the  $\beta$  and  $\gamma$  phases are shown, respectively. The hydrogen content

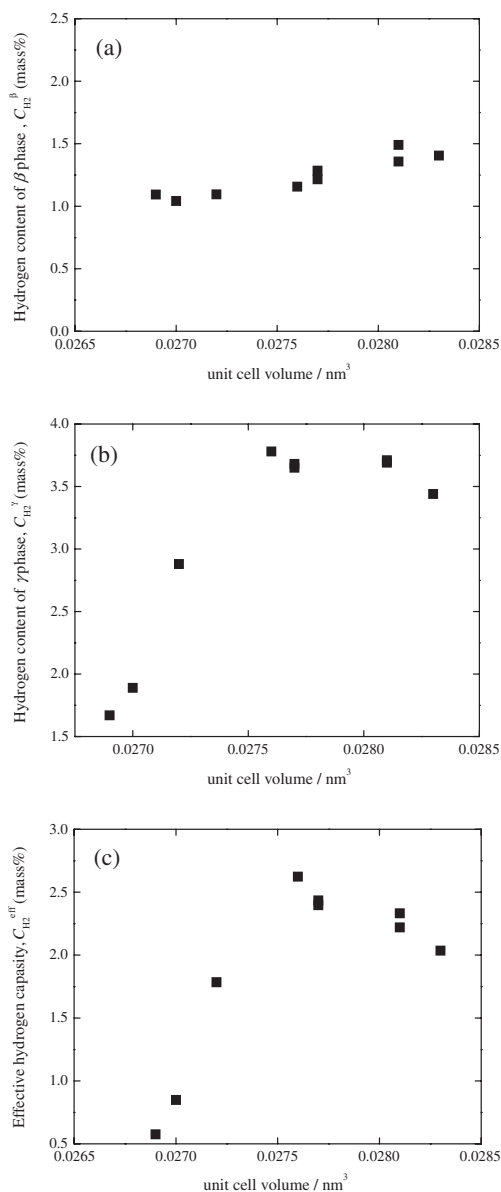


Fig. 5 Graph of content of (a)  $\beta$  phase, (b)  $\gamma$  phase and (c) effective hydrogen capacity on the unit cell volume of dehydrogenated alloys hydrogen.

of the  $\beta$  phase increases slightly with increasing unit cell volume of the  $\alpha$  phase (Fig. 5(a)). In contrast, the hydrogen content of the  $\gamma$  phase increases with increasing unit cell volume of the  $\alpha$  phase and reaches a maximum value around the volume of 0.0275–0.0280 nm<sup>3</sup>, which is nearly equal to that of pure vanadium (0.0278 nm<sup>3</sup>), followed by decreasing of hydrogen capacity of specimen (Fig. 5(b)). As a result, the maximum effective hydrogen capacity (2.62 mass%) is obtained when the unit cell volume is 0.0276 nm<sup>3</sup> (Fig. 5(c)).

#### 4. Conclusions

The vanadium-rich ternary V-Ti-Cr alloy was investigated with the goal of obtaining a large effective hydrogen storage capacity. The hydrogen content of the hydrides with high pressure plateau ( $\gamma$  phase) strongly depends on the unit cell length of the original alloys ( $\alpha$  phase). When the unit cell length of the original alloy is shorter than 0.301 nm, the alloys exhibit a rather small effective hydrogen capacity. In this case, the hydrogen content of the  $\gamma$  phase is small because it contains a monohydride with a FCC structure and a BCC phase with unit cell length shorter than that of the  $\alpha$  phase. When the unit cell length of the original alloy is longer than 0.301 nm, the  $\gamma$  phase mainly consists of the FCC dihydride, similar to pure vanadium. Consequently, the hydrogen content of the  $\gamma$  phase depends strongly on the unit cell length of the  $\alpha$  phase, which is mainly influenced by alloy composition. However, the hydride with low pressure plateau ( $\beta$  phase) forms the BCT phase like pure vanadium, and the hydrogen content depends weakly on alloy composition. As a result, the maximum effective hydrogen capacity (2.62 mass%) is obtained for a unit cell volume of 0.0276 nm<sup>3</sup> (60 at% V-15 at% Ti-25 at% Cr).

#### Acknowledgements

The author gratefully acknowledges the help of Ms Chie Takami with the experiments. This work was supported by a grant from Toyota Motor Corporation.

#### REFERENCES

- 1) D. Mori, K. Hirose, K. Komiya, M. Ishikiriyama, N. Haraikawa, K. Toh, K. Fujita, S. Watanabe, M. Miyahara, S. Mikuriya and M. Tsukahara: Int. Sym. on Metal-Hydrogen Systems, (June 24–28, 2008, Reykjavik).
- 2) J. Reilly and R. H. Wiswall Jr.: Inorg. Chem. **9** (1970) 1678.
- 3) L. Schlapbach and A. Züttel: Nature **414** (2001) 353.
- 4) M. Tsukahara, Y. Kamiya and K. Takahashi: The 14th World Hydrogen Energy Conf., (June 9–13, 2002, Montréal, Canada).
- 5) T. Tamura, A. Kamegawa, H. Takamura and M. Okada: Mater. Trans. **42** (2001) 1862–1865.
- 6) G. G. Libowitz and A. J. Maeland: Mater. Sci. Forum **31** (1988) 177.
- 7) T. Hagi, Y. Sato, M. Yasuda and K. Tanaka: Trans. JIM **28** (1987) 198–204.
- 8) R. L. Zanoewick and W. E. Wallace: J. Chem. Phys. **36** (1962) 2059.
- 9) M. Tsukahara, T. T. Ueda, K. Tanaka, N. Takeichi, H. Tanaka, S. Kikuchi and H. Miyamura: The 16th World Hydrogen Energy Conf., (June 13–17, 2006, Lyon) p. 564.
- 10) N. Takeichi, K. Tanaka, H. Tanaka, T. T. Ueda, M. Tsukahara, H. Miyamura and S. Kikuchi: J. Alloy. Compd. **446–447** (2007) 543.
- 11) C. A. Snavely and D. A. Vaughan: J. Am. Chem. Soc. **71** (1949) 313.
- 12) Y. Kamiya, K. Takahashi, T. Sato and D. Noreus: Collected Abstracts of the 2002 Annual Autumn Meeting of the Japan Inst. Metals (Nov., 2002, Osaka) p. 369.